Effect of Nozzle Shape on Fluid Flow and Heat Transfer characteristics of an Impinging Jet System – A Numerical Study

Usman Allauddin[1] , Naeemullah[1], Patrick G. Verdin[2]

[1] MED, Faculty of MME, NED University of Engineering & Technology, Karachi 75270, Pakistan
[2] Energy & Power, School of Water, Energy & Environment, Cranfield University, Cranfield MK43 0AL, UK

Abstract. Impinging jet is one of the most efficient techniques to achieve a high heat transfer coefficient and is used in many engineering applications. The present study focuses on the effect of nozzle shape on fluid behavior and heat transfer characteristics. For the current investigation, circular, square, rectangular, and elliptical nozzles with identical hydraulic diameters are used with Reynolds number Re ranging from 15,000–35,000. The circular nozzle results are validated with the published numerical and experimental data. In the current study, it is found that as the Reynolds number increases, the value of the averaged Nusselt number increases in all circumstances. When examining the different nozzle shapes, the value of the averaged Nusselt number is higher when an elliptical nozzle is used. The contours of the surface Nusselt number and velocity streamlines are also presented. The contour shows that the heat flux is highest in the stagnation zone and gradually decreases to the sides because they are outside the impingent coverage. Moreover, the area between the jets has a low heat flux. The heat transfer in the impinging zone is initially raised as the jet-induced crossflow increases and achieves a peak value, and then reduced stream-wise because of the crossflow effect.

1 INTRODUCTION

Jet impingement is one of the most efficient methods of cooling hot surfaces or objects in industrial processes because it produces a very high heat transfer rate through forced convection. Since the heat transfer rate is very high at the region where the jet directly impinges on it, provides rapid cooling or heating on the local heat transfer area. Because of its rapid heat removal rates and low-pressure drops, jet impingement is often used for cooling, heating, and drying in a wide range of industrial applications. There are a number of parameters that can affect the heat transfer rate in a jet impingement configuration such as jet type, Nozzle-to-target separation, Nozzle geometry, Reynolds number, etc. For the design and optimization of jet impingement cooling or heating, it is essential that the effect of these parameters of importance must be characterized. For a better understanding of the jet impingement heat transfer processes, the details of flow, geometry and turbulence conditions are required so that a comparison between different experimental data can be

made. Due to the difficulties in performing and comparing experiments, a numerical simulation would have an ideal approach for quantifying the effect of the parameters of interest.

Recently, Barewar et al. [1] and Prevost et al. [2] reviewed different studies aiming at heat transfer enhancement with a major focus on the geometric features of the jet nozzle. Barewar et al. [1] reported that two widely investigated jet nozzle configurations are slot jets and circular jets. This highlights the research required to investigate other nozzle jet configurations. Attalla et al. [3] conducted an experimental investigation on the influence of nozzle geometry on heat transfer uniformity for impinging jet on a smooth surface. They used a square and circular nozzle with a 7.5 mm hydraulic diameter at Reynolds number range from 2,000 to 10,000. They found that the average heat flux for the circular nozzle was 7.8% higher than for the square jet. In contrast, the heat transfer uniformity was improved with the square jet, which was approximately 10.7% higher when compared to a circular jet. They also determined that a rise in Reynolds number improves both the nozzle's pumping force and the heat transfer uniformity. Singh et al. [4] investigated experimentally the impact of nozzle shape on the heat flux from a heated cylinder. The preheated cylinder's surface was kept at a constant temperature. As a working fluid, they used air, and three distinct nozzle geometries, namely circular shape, square, and rectangular shape having identical hydraulic diameters. The Reynolds number, determined by the hydraulic diameter of the jet, varies between 10,000 and 25,000. According to the results, the rectangular jet was found to be more effective at transferring the heat from the cylinder. On the other hand, the cylinder heat flux was more effective when the circular nozzle was used for a constant modified Reynolds number. Gulati et al. [5] conducted an experimental investigation to evaluate the impact of various parameters such as nozzle geometry, the distance between plate to jet, and Reynolds number of air jet impingement. They used round, square, and rectangular-shaped nozzles all about 20 mm in diameter. The distance between the target surface and the jet is 0.5 and 12 mm. Thermographic images were produced using infrared thermal imaging technology to evaluate local heat transfer coefficients. The study found that heat transfer rates enhanced as the Reynolds number increased. They also found that the rectangular shape of the nozzle has a greater Nusselt number distribution than the circular and square jets. Vinze et al. [6] experimentally investigated the impact of the jet exit temperature of the impinging jet on the heat transfer and nozzle geometry on a smooth surface. A thin film approach was used to determine the local wall temperature. The influence of the nozzle's shape on heat flux was investigated using three distinct nozzle shapes: circular, square, and triangular nozzle, with Reynolds number of 5,000, 10,000, 15,000, and 23,000 at various distances from the jet to the plate. From the results, they observed that heat transfer increases by increasing Reynolds number. They also found that a circular nozzle had the highest heat flux than square and triangular nozzles. It was also observed that the temperature of the jet has a minor impact on heat flux. Koseoglu et al. [7] investigated the nozzle configuration and aspect ratio on the rate of heat transfer experimentally and numerically. The following jet exit configurations were examined: circular, elliptical, and rectangular. The temperature was measured using thermal liquid crystal technology. Numerical calculations were also performed. They found that the heat flux in the stagnation zone increases as the aspect ratio increases. Furthermore, aspect ratio and local heat transfer influence decreases as the distance from jet to plate increases. Bachute and Watvisave [8] experimentally investigated the impact of different nozzle shapes in a jet impingement. The nozzles used were circular, square, and rectangular in the Reynolds number range of 5,000 to 15,000. The nozzle's hydraulic diameter was used to determine the size of the nozzle exit area (7 mm). The Reynolds number was found to have the same effect on the performance of heat transfer in all cases as the value of the Reynolds number increased, the resulting Nusselt number also increased. According to the authors'

findings, the heat flux with a square nozzle was more than that of a circular or rectangular nozzle, and the highest heat flux with a square nozzle was achieved. Dano et al. [9] examined experimentally the characteristics of heat transfer and velocity profile of confined impinging jets. Digital Particle Image Velocity Measurement and Flow Visualization approaches were applied to characterize the fluid flow. The Thermocouple Liquid Crystal methods were used to calculate the local heat transfer coefficient. They used cusped ellipse and circular nozzle geometry and reported that the flow evolution from the elliptical jet affects the flow of the wall's region more than the flow of the circular jet due to the crossflow interactions. A cusped ellipse nozzle increases overall heat transfer at the near-surface region at a higher Reynolds number. Marzec et al. [10] studied analytically the characteristics of heat transfer of a system of impingement cooling with various nozzle geometries. An inline arrangement of six impingement jets in a cylindrical plenum was used in the experiment. ANSYS CFX, a CFD tool, was used to perform the simulations. The SST k-ω turbulent model was used in the calculations. According to the results, the chamfer nozzle arrangement had the most significant deflection angle, especially during the first jet. The countersunk nozzle had the lowest drop in pressure during the investigation. They found that the sudden rise in flow rate when it reached the nozzle was the source of the significant pressure drop for a cylindrical nozzle. Tomaso and Nino [11] studied the experimental and numerical characteristics of the jet flow produced by a square nozzle using the Particle Image Velocity Measurement approach. The target plate was kept at a constant temperature. Numerical simulations were also performed using the CFD tool. The measured and calculated airflow profiles were found to be in excellent agreement. For the smallest aspect ratio, the results showed that the Richardson number has a moderate effect on the flow formation generated in all Reynolds number.

The literature review of the current work shows that the performance of the impinging jet system is a function of a variety of parameters. To the best of the authors' knowledge, no comprehensive study is reported in open literature investigating the effect of a variety of nozzle shapes in multiple impinging jet systems of industrial importance. The current research work addresses this research gap.

2 GOVERNING EQUATIONS

In this study, for the CFD simulation, ANSYS-FLUENT version 16.0 is used. Computational fluid dynamics CFD is a computer-based approach for simulating system behaviour that includes physical processes such as fluid flow, heat transfer, etc. It performs by resolving fluid dynamic equations in a specified form over a specified region while considering a set of boundary conditions. CFD has been used in key sectors because of its ability to solve multiple system parameters at a lower cost than an experimental investigation. The three-dimensional governing equations of mass, momentum, and energy in a steady-state turbulent flow are as follows:

The continuity equation:

$$\frac{\partial \overline{u}_i}{\partial x_i} = 0 \tag{1}$$

The momentum equation:

$$\frac{\partial(\rho U_j U_i)}{\partial x_i} = -\frac{\partial \rho}{\partial x_i} + \frac{\partial}{\partial x_j}\left[\mu\left(\frac{\partial U_i}{\partial x_j} + \frac{\partial U_j}{\partial x_i}\right) - \rho\overline{\acute{U}_i \acute{U}_j}\right] \tag{2}$$

The energy equation:

$$\frac{\partial(\rho U_i T)}{\partial x_i} = \frac{\partial}{\partial x_i}\left[k\frac{\partial T}{\partial x_i} - \rho C_p \overline{\acute{U}_i \acute{T}}\right] \tag{3}$$

Here T, P, Ui, μ and ρ, signify average temperature, pressure, velocity element, dynamic viscosity, and fluid density, correspondingly, whereas Ui′ and T ′ denote velocity components in the xi-coordinate direction and changing temperature, respectively. There are several turbulence modelling options, including k–ε and k–ω models. The SST (shear stress transport) k–ω model is a combination of k–ε and k–ω models (Menter [12]), which is used by many researchers for numerical studies of jet impingement processes. Because of its significantly improved accuracy and faster processing time, the SST k–ω model was chosen (Peng et al. [13], Zu et al. [14], Allauddin et al. [15], Allauddin et al. [16], Allauddin et al. [17]). Moreover, this model outperformed the other turbulence models in stagnation regions in predicting turbulent kinetic energy values. Thus, this type of model is employed for all simulations in this work. The SST k–ω model performs computations using the k–ω for fluid flow close to the wall and the k–ε model for fluid flow distant from the wall.

3 NUMERICAL SETUP

The computational domain used in the current work is a rectangular channel taken from an array of a multiple-jets impingement systems. A row of nine impinging jet is simulated utilising the symmetry of the geometry. The hydraulic diameter of nozzle (D_h), Nozzle to nozzle spacing (X), Impingement plate Length (L) and Nozzle to plate spacing (H) are 10 mm, 50 mm, 525 mm and 30 mm, respectively. The computational domain dimensions exactly match the experimental work of Wan et al. [18]. The design model of the jet impingement systems with circular, square, rectangular, and elliptical nozzles is shown in Figure 1. All other parameters are kept constant and just nozzle shapes are changed to study the nozzle shape effect while the hydraulic diameter of all shapes is kept constant.

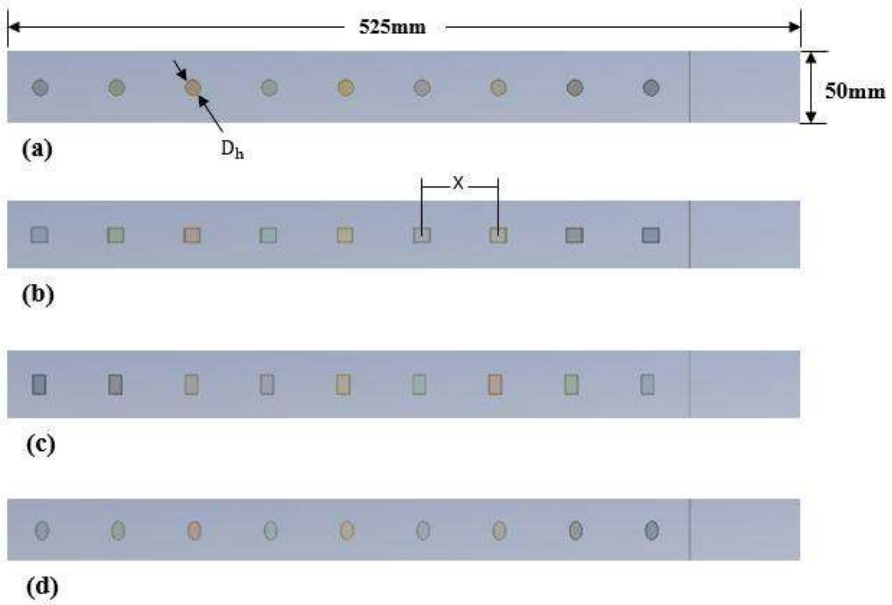

Fig. 1. Schematic view of computation domains using various nozzle shapes: (a) Circular nozzle (b) Square nozzle (c) Rectangular nozzle (d) Elliptical nozzle

The computational domain along with the boundary conditions used in the current work is shown in Figure 2. The details of the boundary conditions are tabulated in Table 1. The extended region of 75 mm is used to make sure that the outlet boundary condition does not affect the internal flow and also to ensure stability during numerical simulations. A view of the computational mesh is shown in Figure 3 along with the zoomed regions showing wall inflations and mesh refinement in the critical regions of the flow.

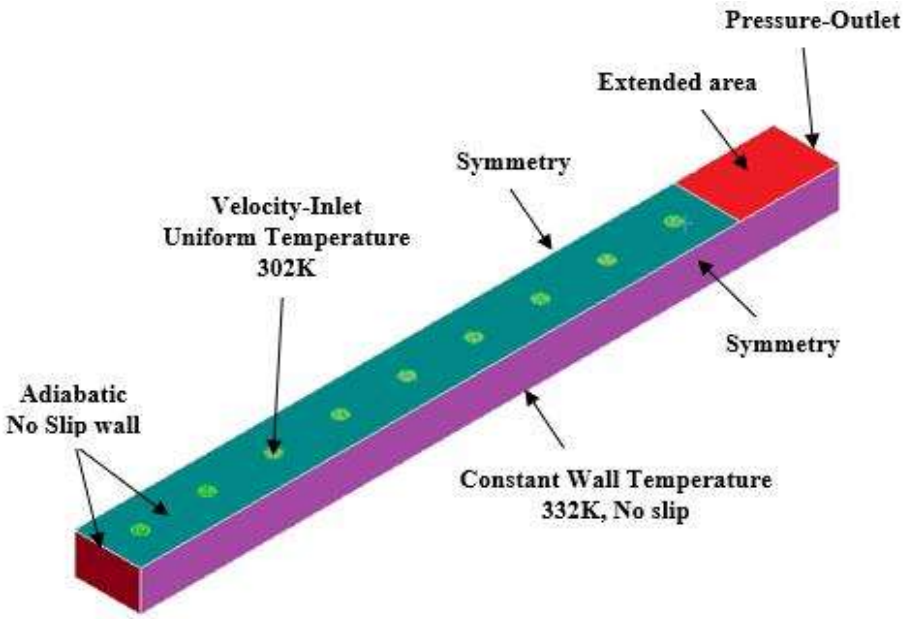

Fig. 2. Computational domain along with the boundary conditions

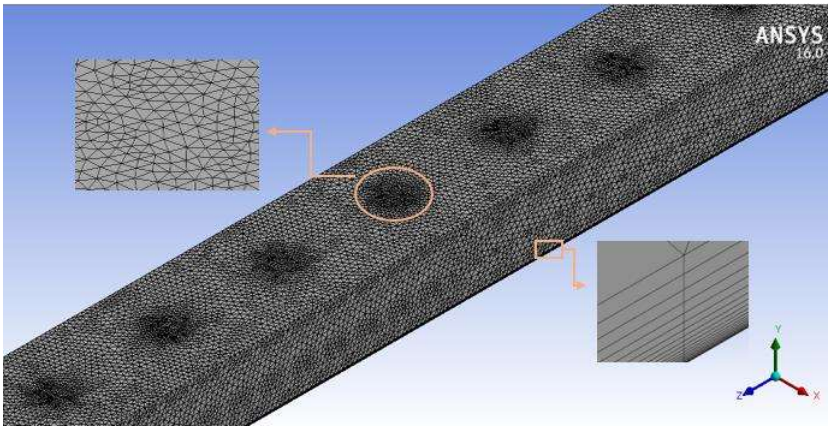

Fig. 3. Schematic view of the computation mesh

Table 1.

General	**Solver:** Pressure-based, Steady
Model	**Energy equation**: On k-ω SST model with default quantities
Material	Air with default properties (with standard thermal properties)
Operating pressure	101,325 Pa
Boundary conditions	**inlets:** Velocity-inlet with 302K (Velocity computed from Re) **Turbulence:** 5% turbulent intensity **Top plate:** No slip, adiabatic wall **Outlet:** Pressure-outlet (0-gauge pressure with 302K) **Target plate:** No slip, constant temp: 332K **Side Walls:** Symmetry **Wall opposite the outlet wall:** No-slip, adiabatic wall
Solution Methods	SIMPLE scheme
Spatial Discretization	Second-order upwind for every equation

For the sake of brevity, the details of different options (solver, energy model, turbulence model, material, operating pressure, boundary conditions, pressure velocity coupling and discretization schemes) selected during the case setup of the numerical simulations are tabulated in Table 1.

The following expression is used to estimate the Jet Reynolds number (Re):

$$Re = \frac{\rho V D_h}{\mu} \tag{4}$$

Here D_h and V are the hydraulic diameter and velocity of the jet at inlet, respectively. The following expression is used to estimate the value of Nusselt number (Nu):

$$Nu = \frac{\dot{Q}}{A(T_w - T_j)} \frac{D_h}{k} \tag{5}$$

The $\dot{Q}$, A, T_j, and T_w denote the heat flux, target plate's area, temperature of jet at inlet and target plate temperature, respectively, while k denotes the thermal conductivity of air at the temperature of the jet's inlet.

4 Results and Discussion

The findings of the current investigation are presented in this section. For model validation, previous CFD and experimental data will be used to compare the current CFD results for a circular nozzle at Re = 35,000. The impact of nozzle shape on fluid flow and characteristics of heat transfer of an impinging jet system will be then investigated by using various nozzle shapes including square, rectangular, and elliptical shape nozzle. The effect of various Reynolds number Re in the range of 15,000–35,000 will also be examined.

4.1 Grid Independency study

If the mesh refinement is not good enough, it can lead to discretization errors. The grid convergence index (GCI) technique plays a vital role in correcting these errors. It is common practice to use the GCI technique in RANS-based computational fluid dynamics (CFD) simulations to measure and eliminate discretization errors. This technique is based on the generalized theory of Richardson extrapolation. Three unstructured grids with tetrahedral elements were systematically refined with a refinement ratio of about 1.6. On the target wall, inflation layers are used for near-wall modelling. The number of inflation layers in the grids is 20 with prism elements and a growth rate of 1.2. Furthermore, because the SST k-ω model is being applied, the near-wall grid quality had to be ensured. Therefore, the value of the y+ factor, the distance between the first node and the wall, has to be lower than one. A schematic view of the fine grid is presented in Figure 3. At a Reynolds number of 35,000, the grid independence analysis is carried out on the circular nozzle. The grids used for the grid dependence study are listed in Table 2. The coarse, medium and fine grids are systematically refined of 465,397, 857,224, and 161,452,0 elements. The change in averaged-Nusselt number values with grid refinement is not significant. On the fine, medium, and coarse girds, the average Nusselt number values are 100.471, 100.300, and 100.115, respectively. The average Nusselt number difference between coarse and fine grids is less than 0.4%. All grids have y + value lower than 1.0. The fine grid has a 1.93% grid convergence index, indicating that a numerical error is only 1.93% for the average Nusselt number; hence, the medium grid is selected for the subsequent computations, based on the grid independence analysis.

Table 2. Results of grid independence analysis.

	Grid	**Number of elements**	$\mathbf{Nu_{avg}}$	**y +**	$\mathbf{GCI}_{fine}$
Circular Nozzle	coarse	465,397	100.115	0.389	1.93%
	medium	857,224	100.300	0.395	
	fine	1,614,520	100.471	0.395	

4.2 Model Validation

Figure 4 compares the current CFD Nusselt number contours of the circular nozzle at Re = 35,000 with the past CFD and experimental data from Wan et al. [18] and Xing et al. [19]. It is found that the present CFD results are similar to those in previous CFD and experimental results. The Nusselt number contours in this numerical analysis have similar spreading behavior as in the published data. The highest values of Nusselt number are found at the centerline (i.e., stagnation zone) of the target plate because the intensity of the jet is more significant in the stagnation zone, and the jet-induced crossflow is insignificant. Nusselt number values rapidly decline as it moves away from the point of stagnation. In the region between the jets, the Nu are low due to jet interaction and crossflow. Furthermore, the upstream zone has a large value of the surface Nusselt number. However, due to working fluid acceleration, it is comparably low at the downstream. Figure 5 compares the average Nusselt number for circular nozzles. In this case, Reynolds number range from 15,000 to 35,000 with past data of Wan et al. [18], Xing et al. [19], and El-Gabry et al. [20]. and. The results of the current simulation closely match the experimental data. This confirms that the current model is valid. Thus, a similar model is employed to determine heat transfer characteristics and fluid flow on other nozzle shapes.

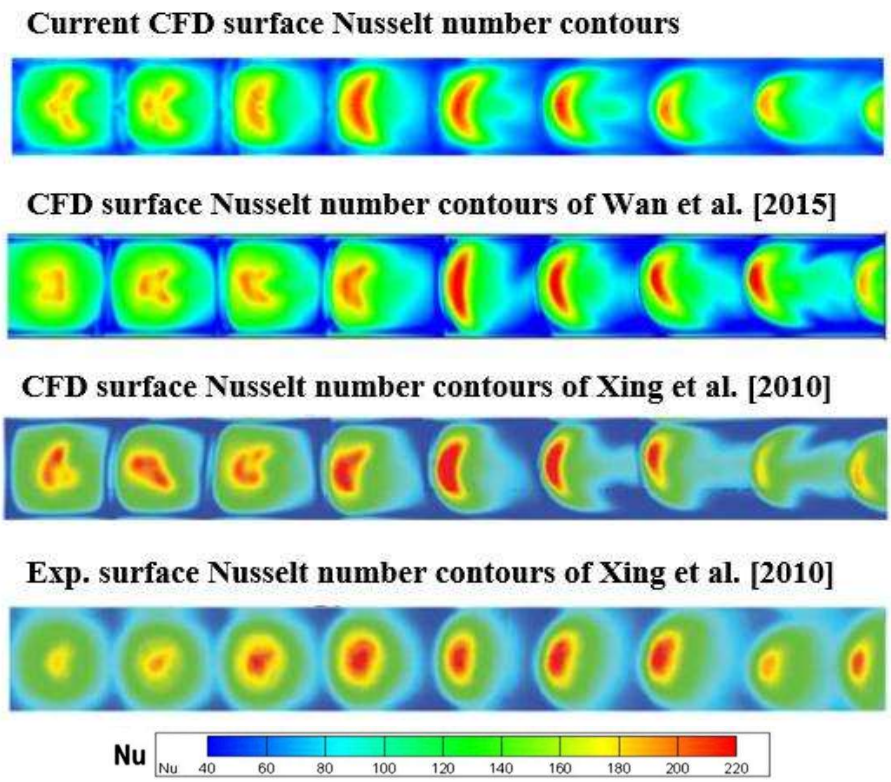

Fig. 4. Comparison of current CFD results of Nusselt number contours of a circular nozzle with literature data Re = 35,000

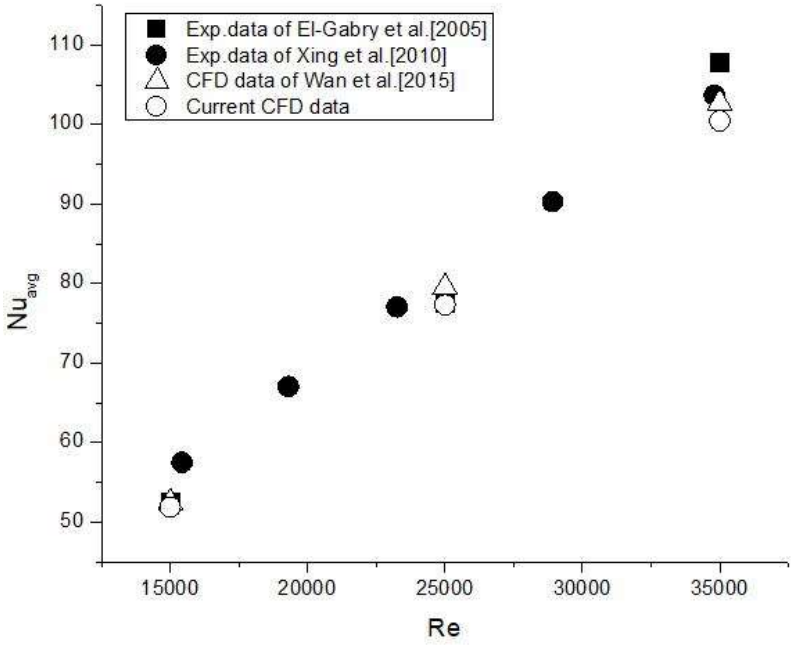

Fig. 5. Comparison of current CFD values of averaged Nusselt number with the literature data

4.3 Flow Field results

Figure 6 shows the comparison of the streamlines and velocity distributions at $\boldsymbol{Re}$ = 35,000 using various nozzle shapes (circular, square, rectangular, and elliptical). Figure 6a presents the streamlines and velocity distributions in the central plane (at 5D/2 width of the channel). In contrast, Figure 6b depicts the streamlines and velocity distributions on the plane, close to the wall (at 5D/4 width of the channel). The jets in all four cases can be observed to be progressively bent along the direction of flow. This phenomenon is caused by crossflow. In the general analysis of the flow dynamics of the multiple jets shown in Figure 6, it is found that the air flowed through the nozzles at a high velocity and started to mix with the surrounding air. This is referred to as the "free jet region." Jet flow and ambient air were mixed, creating a shear layer that resulted in large velocity gradients. This implies the identification of fully developed zones. The axial velocity of the jets dropped as they approached the wall, and it was changed into an accelerated horizontal component. This was identified as the stagnation region, which had a thin boundary layer and a greater static pressure. The flow velocity was increased along the plate from zero to a maximum at a particular distance from the stagnation point as the flow developed over the target plate. Higher heat transfer coefficients are expected in the vicinity of the stagnation region due to this jet flow configuration, although a portion of the wall jet region significantly contributed to the heat exchange. As shown in Figure 6, the jets' interactions upstream and downstream of the impingement increased the flow complexity. The amount of the crossflow formed by the upstream jet flow is seen near the outlets, indicating the increased flow velocity.

All of the jets behave in the same way, with constant axial flow rates in the jet zone. The red contours represent high-velocity regions. At the strike of the jet, it creates stagnation regions on the target plate and redirects the axial flow to the direction of the wall jet. Vortex formations occur around the stagnation zones during the first few impinging jets. The impinging jets are directed towards the channel's downstream end, when the distance between the jets increases. At the downstream end, the flow is increased, and the vortexes are eliminated. Low-velocity zones with high-velocity jets impinging can be observed through channels about a length of < L /2. When length > L/2, crossflow effects are noticeable. The flow acceleration produced by crossflow appears as the distance in the outflow side increases. The heat transfer rates in these zones are affected by the flow acceleration generated by the crossflow in the downstream zone, which will be explained in the coming section.

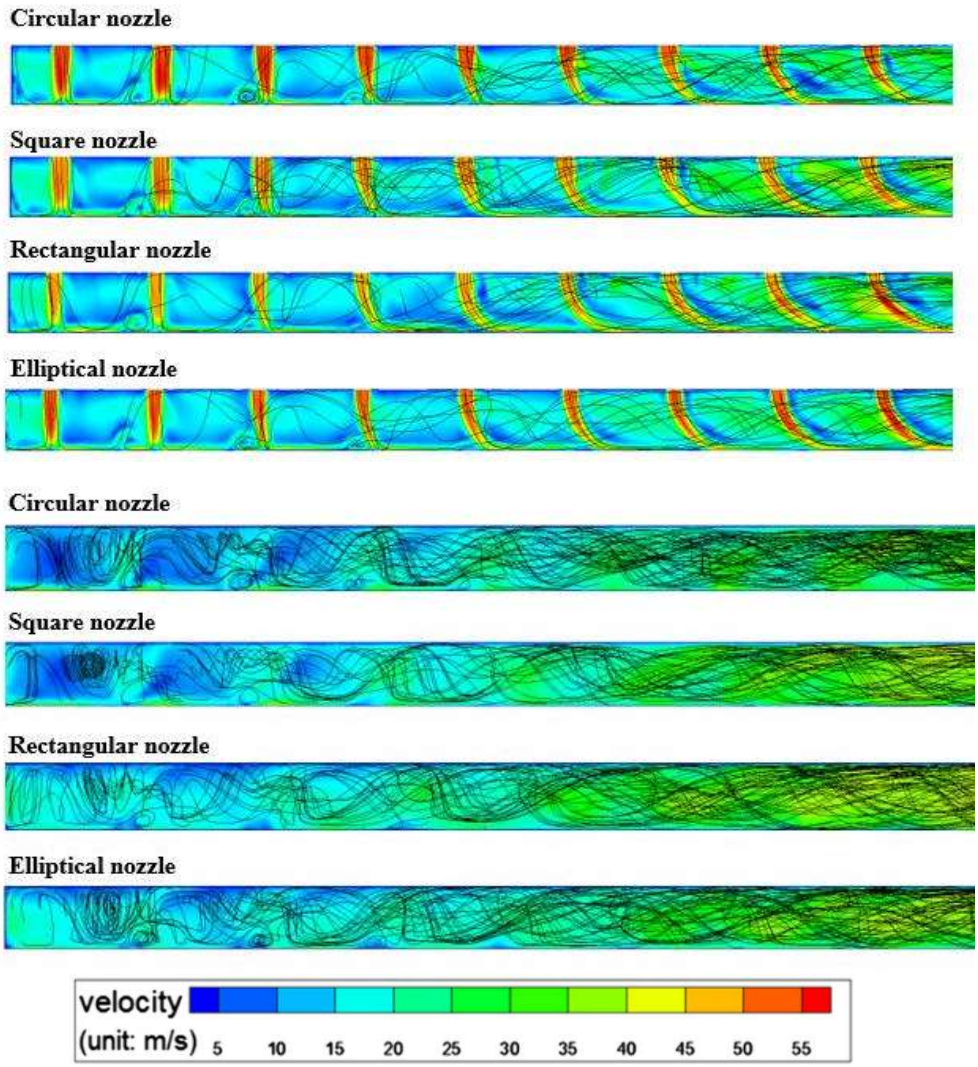

Fig. 6. Velocity contours with streamlines for the cases of circular, square, rectangular, and elliptical nozzles at Re = 35,000 along: (a) Centre of plane and (b) Near the wall plane

4.4 Heat transfer results

The surface Nusselt number contours for the circular, square, rectangular, and elliptical shape nozzles are shown in Figure 7 at Re = 35,000. The Nusselt number is defined as convective to conductive heat transfer ratio. The red color contours represent the high Nu values in Figure 7. The impingement jet positions are visible in the contours of the surface Nusselt number. The heat flux is highest at the point of stagnation and decreases rapidly to the sides. The space between the jets had a low heat transfer rate since it was not covered by jet impingement. In the region of impingement, the heat flux increases upstream (jets 1-4), but further downstream showed less heat flux in the target plate as the crossflow increased, preventing the jet impinging on the target surface. The heat transfer value is lower outside of the jet coverage due to the spreading of the wall jet and crossflow. The self-induced crossflow interrupts other wall jets, moves stagnation points, and forms thicker boundary layers, decreasing averaged heat transfer rates.

The heat transfer non-uniformity on the target plate appears to be influenced by the nozzle shapes. The induced higher velocities in the vicinity of the target plate increase the overall turbulence of the flow. This increased turbulence would enhance the heat transfer rates compared with the various shapes of nozzles. As the wall jet induced by the jet went through the outlet, they collided with the wall jets. This led to a decrease in the impingement area, and a reduced local heat transfer in that region. Figure 8 depicts the averaged Nusselt number of the different nozzle shapes at various Reynolds number (15,000, 25,000, and 35,000). In all cases, as Reynolds number increases, the averaged Nusselt number increases. On the other hand, circular and elliptical nozzles produce notably higher Nusselt number than other nozzle shapes. At a Reynolds number of 35,000, circular, square, rectangular, and elliptical nozzle values are approximately 100.47, 96.44, 99.21, and 101.70, respectively. As a result, the shape of the nozzle has a considerable impact on its heat transfer performance. Thus, for the flat plate jet impingement system, an elliptical nozzle is found to be more effective.

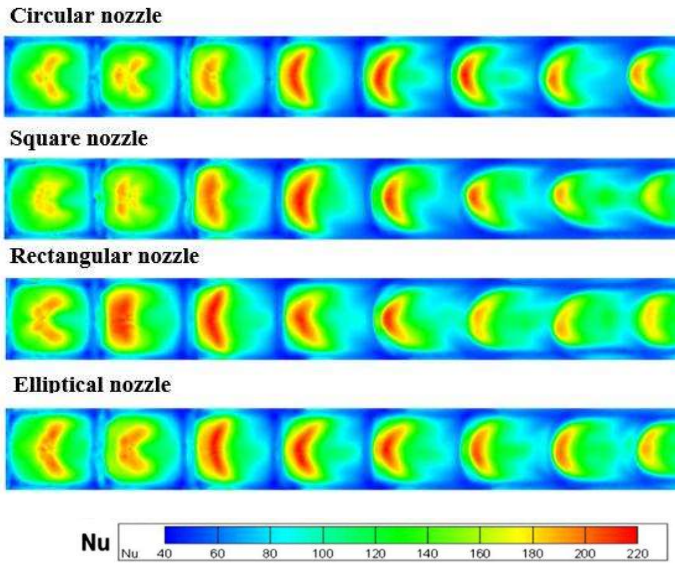

Fig. 7. CFD contours of Nusselt number with circular, square, rectangular, and elliptical nozzles at Re = 35,000

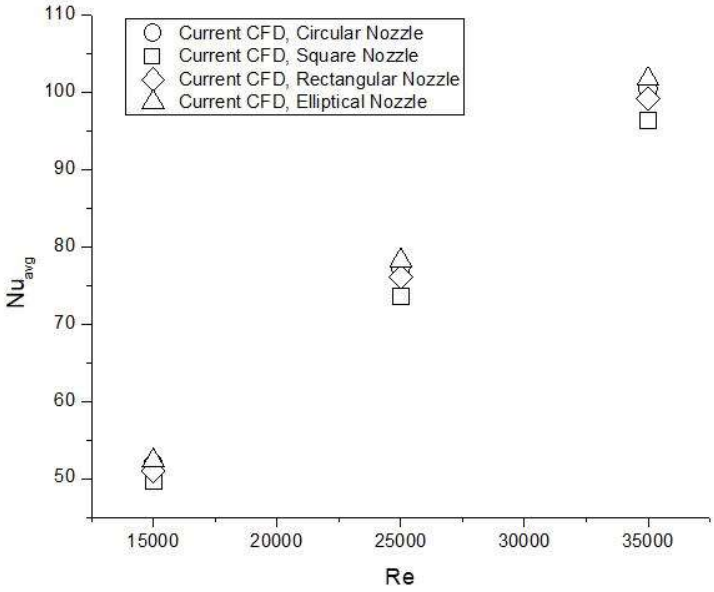

Fig. 8. Comparison of averaged Nusselt number values with circular, square, rectangular, and elliptical nozzles

5 CONCLUSION

The effect of the nozzle shapes on the multiple jets impingement system is investigated using four various nozzle configurations: circular, square, rectangular, and elliptical nozzle. The effects of various Reynolds number on the averaged Nusselt number are also investigated. The current solutions of the circular jet impingement are validated using past experimental and numerical data. After that, the validated design model is employed to estimate the behavior of fluid and heat transfer characteristics of the impinging jet with various nozzle shapes. The following are the conclusion of the present study:

- The resulting velocity streamlines presented the numerous detailed flow characteristics, including nozzle-induced flow redirection, surface-flow collisions, vortex rings, across the stagnation point, and vortex caused by the crossflow, which all helped in the understanding the mechanism of heat transfer in jet impingement on various nozzle shapes.
- In the analysis of heat transfer, the impact of various nozzle shapes on thermal performance was investigated through contours of surface Nusselt number, which helps to understand the jet impingement cooling mechanism.
- The multiple jet impingements on the flat pale by elliptical nozzle performed better than the other nozzle shapes.

The Orientation of nozzles might also be effective in heat transfer processes. The effect of the swirl induced by obstacles in nozzles can also be investigated to find the effect on fluid flow and heat transfer characteristics. The target surface can also be roughened with different surface enlargement elements.

References

1. S. D. Barewar, M. Joshi, P. O. Sharma, P. S. Kalos, Optimization of jet impingement heat transfer: A review on advanced techniques and parameters, Thermal Science and Engineering Progress, **39**, 101697 (2023).
2. T. Prevost, S. Battaglioli, R. Jenkins, A.J. Robinson, Enhancing Jet Array Heat Transfer: Review of Geometric Features of Nozzle and Target Plates, International Journal of Thermofluids, **16,** 100203, (2022).
3. M. A. Hussein, M. Maghrabie, A. Qayyum, A. G. Al-Hasnawi, E. Specht, Influence of the nozzle shape on heat transfer uniformity for an inline array of impinging air jets, Applied Thermal Engineering, **120**, 160–169, (2017).
4. D. Singh, B. Premachandran, S. Kohli, Effect of nozzle shape on jet impingement heat transfer from a circular cylinder, International Journal of Thermal Sciences, **96**, 45-69, (2015).
5. P. Gulati, V. Katti, S.V. Prabhu, Influence of the shape of the nozzle on local heat transfer distribution between a smooth flat surface and impinging air jet, International Journal of Thermal Sciences, **48**, 602–617, (2009).
6. R. Vinze, S. Chandel, M.D. Limaye, S.V. Prabhu, Influence of jet temperature and nozzle shape on the heat transfer distribution between a smooth plate and impinging air jets, International Journal of Thermal Sciences, **99**, 136-151, (2016).
7. M.F. Koseoglu, S. Baskaya, The role of jet inlet geometry in impinging jet heat transfer, modelling, and experiments. International Journal of Thermal Sciences, **49**, 1417-1426, (2010).
8. B. Bachute and D. S. Watvisave, Experimental Study of Influence of Different Nozzle Configuration on a Heat Transfer in Jet Impingement, International Journal of Current Engineering and Technology, **5**, 78-81, (2016).
9. B. P. E. Dano, J. A. Liburdy, K. Kanokjaruvijit, Flow characteristics and heat transfer performances of a semi-confined impinging array of jets: Effect of nozzle geometry. International Journal of Heat and Mass Transfer, **48**, 691–701, (2005).
10. K. Marzec, and A Kucaba-Pieta, Heat transfer characteristic of an impingement cooling system with different nozzle geometry, Journal of Physics: Conference Series **530**, 012038, (2014).
11. R. M. D. Tommaso, E. Nino, Investigation on an Impinging Square Jet, International Journal of Modern Engineering Research, **07**, 05–14, (2016).
12. F. R. Menter Two-equation eddy-viscosity turbulence models for engineering applications, AIAA J., (1994).

    32(8):1598-1605.
13. W. Peng, L. Jizu , B. Minli, W. Yuyan, H. Chengzhi, A numerical investigation of impinging jet cooling with nanofluids, Nanoscale Microscale Thermophys Eng., **18**, 329-353, (2014).
14. Y. Q. Zu, Y. Y. Yan, J. D. Maltson, CFD prediction for multi-jet impingement heat transfer, Proceedings of Turbo Expo: Power for Land, Sea and Air. Orlando, FL, (2010).
15. U Allauddin, N. Uddin, S.O. Neumann, Heat Transfer Enhancement by Detached-Ribs on a Surface Subjected to Jet Impingement, Journal of Thermophysics and Heat Transfer, **27**, 355-360, (2010).

16. U. Allauddin, R. Mohiuddin, H. M. Usman Khan, N. Uddin, W. A. Khan, Nanoscale heat transfer investigation of an array of impinging jet systems with different working fluids under crossflow with and without pin fins, Heat Transfer, **50**, 81-104, (2021).
17. U. Allauddin, M. U. Sohail, M. Sohaib, M. A. Siddiqui, M. H. U. Khan, K. Khan, P. G. Verdin, Heat transfer enhancement investigation in jet impingement system of a single and array of square jets using numerical tools, Computational Thermal Sciences: An International Journal, 15(4), (2023).
18. C. Wan, Y. Rao, P. Chen, Numerical Predictions of Jet Impingement Heat Transfer on Square Pin-Fin Roughened Plates, Appl. Therm. Eng., **80**, 301–309, (2015).
19. Y. Xing, S. Spring, B. Weigand, Experimental and Numerical Investigation of Heat Transfer Characteristics of Inline and Staggered Arrays of Impinging Jets, J. Heat Transf., **132**, 092201, (2010).
20. L. A. El-Gabry, D. A. Kaminski, Experimental Investigation of Local Heat Transfer distribution on smooth and roughened surfaces under an array of angled impinging jets, J. Turbomach., **127**, 532–544, (2005).

Effect of nozzle shape on fluid flow and heat transfer characteristics of an impinging jet system – a numerical study

Allauddin, Usman

2024-06-25

Allauddin U, Naeemullah, Verdin PG. (2024) Effect of nozzle shape on fluid flow and heat transfer characteristics of an impinging jet system – a numerical study. In: 2nd International Conference on Modern Technologies in Mechanical & Materials Engineering (MTME-2024), 20 April 2024, GIK Institute of Engineering Sciences and Technology, Topi, Pakistan, Volume 398, Paper number 01004

https://doi.org/10.1051/matecconf/202439801004